TIME DEPENDENT CRITICAL STATE IN DISKS AND RINGS

H. Hemmes, A.R. Kuper, and L.J.M. van de Klundert

University of Twente, Department of Applied Physics,
P.O. Box 217, 7500 AE Enschede, The Netherlands.

Abstract

We have developed a model to calculate the response of the current distribution in disks and rings to a time dependent applied magnetic field. In the model the ring (or disk) is divided in concentric segments. The segments are assumed to be inductively coupled to each other and to the applied field. A time dependent magnetic field induces a finite electric field in the ring/disk.The induced currents will then depend on the magnitude of the electric field and the current-voltage characteristic. The current-voltage characteristic is modelled by a non-linear resistivity. The currents determined from AC magnetization measurements on rings and experimental I-V characteristics are compared with the results of our model. We find that we can easily reproduce the shape of the magnetization curves. However, the frequency dependence of the current in the rings shows a discrepancy. The experimental frequency dependence of the currents is much smaller than that expected on the basis of the I-V characteristics and the model calculations. A possible cause could be inhomogeneities in the sample, influencing the current distribution.

Introduction

For High Temperature Superconductors, where the preparation of good electrical contacts is not trivial, contactless techniques for the determination of the critical current density are important. Both AC and DC magnetization techniques are used for this purpose. The analysis of the results in terms of critical current density J_c is based on the critical state model [1,2]. Frankel [3] and recently Däumling and Larbalastier [4] applied the critical state model to the determination of J_c from the magnetic field profile in disk shaped superconductors. The finite element technique used by these authors makes it possible to calculate the currents and fields selfconsistently for any finite shape with axial symmetry.

Theory

The model developed in this section describes the response of ring shaped superconducting samples to a time dependent applied magnetic field B_a. The ring has an inner(outer) radius $R_{in}(R_{out})$ and a thickness d. A disk is the special case of a ring with zero inner radius. For the purpose of our calculations we divide the ring into segments, as shown in Fig. 1. Each segment i consists of a loop with radius r_i and cross-section $A_i = \Delta r_i \Delta z_i$, where $\Delta r_i(\Delta z_i)$ is the thickness(height) of segment i in the r(z)-direction. The segment carries a current density J_i. The total current carried by the segment is given by $I_i = J_i A_i$.

Manuscript received September 24, 1990

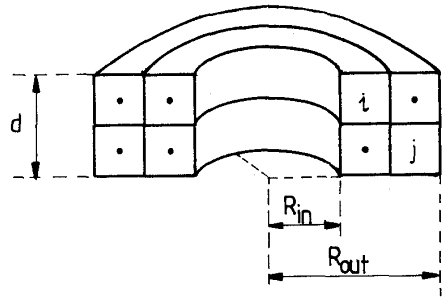

Figure 1. Division in segments of a ring with inner(outer) radius $R_{in}(R_{out})$ and thickness d.

Selffield effects

The current density J_i in segment i is limited by the field dependent critical current density J_c. For the calculations in this paper the field dependence of J_c is described using a Kim relation: $J_c(B) = J_{co}/(1 + |B/B_o|)$. Here J_{co} is the critical current density at zero field, B_o is a scaling field that determines the sensitivity of J_c to the applied local field B. In segment i J_c is determined by the local field B_i.

The current I_j in segment j generates a magnetic field B_{ij} at segment i. It has a z- and r-component: $B^r_{ij} = \beta^r_{ij} I_j$, $B^z_{ij} = \beta^z_{ij} I_j$, both proportional to I_j. If we assume the currents I_j to be running in the center of the segment they form a linear current loop. The loop is centered at r=0 and $z=z_i$. In this case β can be calculated directly by [5]

$$\beta^r_{ij} = \frac{\mu_o}{2\pi} \frac{z_i - z_j}{r_i[(r_i+r_j)^2 + (z_i-z_j)^2]^{1/2}} \times \left(-K(k) + \lambda E(k)\right) \quad (1)$$

$$\beta^z_{ij} = \frac{\mu_o}{2\pi} \frac{1}{[(r_i+r_j)^2 + (z_i-z_j)^2]^{1/2}} \times \left(K(k) + \gamma E(k)\right) \quad (2)$$

with $k^2 = 4r_i r_j/[(r_i+r_j)^2+(z_i-z_j)^2]$,

$$\lambda = \frac{r_j^2 + r_i^2 + (z_i-z_j)^2}{(r_j-r_i)^2 + (z_i-z_j)^2} \text{ and } \gamma = \frac{r_j^2 - r_i^2 - (z_i-z_j)^2}{(r_j-r_i)^2 + (z_i-z_j)^2}.$$

K(k) and E(k) are complete elliptic integrals of the first and second kind.

The magnetic field at segment i (B_i) is the sum of the applied field and the contributions of all other segments

$$B^r_i = B^r_a + \sum_j \beta^r_{ij} I_j, \quad (3)$$

$$B^z_i = B^z_a + \sum_j \beta^z_{ij} I_j, \quad (4)$$

$$B_i = (B^r_i B^r_i + B^z_i B^z_i)^{1/2} \quad (5)$$

0018-9464/91/0300-1069$01.00

The field contribution of segment i itself is taken to be zero (i.e. $\beta^r_{ii} = \beta^z_{ii} = 0$).

Static current distribution

To calculate J_i we need a relation that fixes the magnitude of J_i. Such a relation is provided by the critical state model: $J_i{=}J_c(B_i)$. Now we can solve the currents and fields selfconsistently. Once the current distribution is known the magnetic moment and field distribution can be calculated. This is essentially the model used by Frankel [3] and Däumling and Larbalestier [4] for the calculation of field profiles and magnetization of disk shaped superconductors with a static current distribution.

Dynamic current distribution

Now we will extend the model to include the time dependence of the current distribution. Assuming that all segments are inductively coupled, we have:

$$M_{ii}\dot{I}_i + R_i I_i = -M_{if}\dot{I}_f - \sum_j M_{ij}\dot{I}_j \qquad (6)$$

where M_{ii} is the self-inductance, R_i the resistance and I_i and $\dot{I}_i$ are the current and its time derivative of segment i. M_{if} is the mutual inductance between segment i and the field coil, $\dot{I}_f$ is the time derivative of the current in the field coil and M_{ij} is the mutual inductance between segment i and j. $\phi_i = M_{if}I_f$ is the flux generated by the field coil through segment i. For a homogeneous applied field the flux is also given by $\phi_i = B_a A_i$. The resistance is given by $R_i = \rho_i 2\pi r_i/A_i$, with ρ_i the resistivity, r_i the radius and A_i the cross section of segment i.

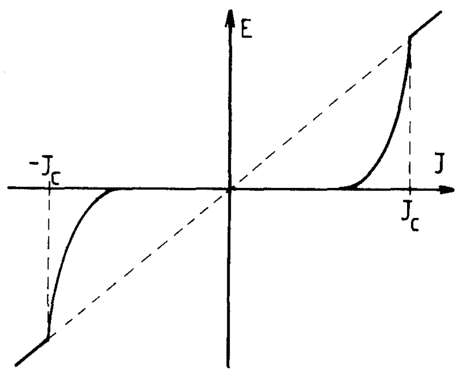

Figure 2. Constitutive equation for a non-ideal superconductor: $E = \rho J$, with ρ a non-linear function of J.

For the calculation of the time dependent currents we use the constitutive equation shown in Fig. 2. The electric field is a continuous non-linear function of the current. This is modelled by a non-linear current dependent resistivity ρ_i for each segment: $E_i = \rho_i J_i$. We use the following expression for the resistivity ρ_i:

$$\rho_i = \begin{cases} \rho_n (J_i/J_c(B_i))^n & J_i \le J_c(B_i) \\ \rho_n & J_i > J_c(B_i). \end{cases} \qquad (7)$$

with ρ_n the normal state resistivity, J_i the current density I_i/A_i and $J_c(B_i)$ a scaling current, playing the role of a "critical current density" that depends on the local magnetic field B_i. The power n determines the steepness of the current-voltage characteristic. In the limit of large n the scaling current <u>is</u> the critical current.

If we plotted $\log(E_i)$ against $\log(J_i)$ using Eq. 7 for ρ_i with a constant J_c, we would find a straight line with slope n+1. However, for the systems we want to study J_c depends on the local magnetic field B_i. An increase of the current in the ring will increase B_i and consequently decrease $J_c(B_i)$. As a result the increase in ρ_i for a given increase in J_i is larger than would be expected from the power n in Eq. 7 alone. A plot of $\log(E_i)$ against $\log(J_i)$ using a field dependent J_c still gives an approximately straight line for the currents and voltages of interest (see also Fig. 7). However the slope, with value $n_{eff}+1$, is larger than the value, n+1, obtained for constant J_c. From the value of this slope we can write for the effective current dependence of the resistivity: $\rho \propto J^{n_{eff}}$.

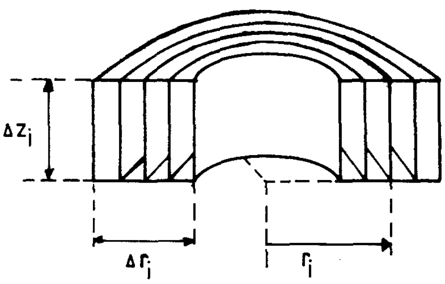

Figure 3. Distribution of cylindrical currents over the cross section of a segment with radius r_i.

Mutual inductances

The mutual inductances M_{ij} between the segments are calculated assuming a homogeneous current distribution in the the segments. The homogeneous current distribution is approximated by distributing several cylindrical currents evenly over the cross section of the segment, as shown in Fig. 3. By increasing the number of cylindrical currents a better approximation of the homogeneous distribution is obtained. The mutual inductance between two cylindrical currents is calculated, within arbitrary precision, using the formalism of Fawzi and Burke [6]. M_{ij} is then obtained by adding all the mutual inductances between the cylindical currents in segment i and j. For our rings $\Delta r_i \ll r_i$ and consequently only a few cylindrical currents are needed to get a good approximation for M_{ij}.

Numerical solution of the currents

The numerical solution of Eq. 6 is straightforward. The time derivatives $\dot{I}_i$ are approximated by a three point backward difference method. Substitution in Eq. 6 gives us with a set of equations in I_i. This set of equations is linear, apart from the terms containing $I_i R_i$. In order to solve this set of equations an iterative procedure is used. A solution I_i^0 is estimated and used to calculate $R_i^0 = R_i(I_i^0)$. Substituting this value for R_i we get a linear set of equations in I_i that can be solved with a resulting solution I_i^1. This is then used as an estimate for the next iteration step which is repeated until the solution has converged. If R_i is a strongly non-linear function of I_i, it is useful to linearize $I_i R_i$: $I_i^1 R_i^1 = I_i^0 R_i^0 + (I_i^1 - I_i^0)\partial R_i/\partial I_i(I_i^0)$. The derivative term dampens the response of I_i^1 if the estimate I_i^0 is not a good one and it disappears when the solution converges.

Experimental

AC magnetization measurements have been performed on YBaCuO rings with an inner radius of 12.5 mm, an outer radius of 14.5 mm and a thicknes of 2 mm. The ring is placed in a field coil. The AC magnetic field generated by this coil induces a current in the ring. A pick up coil is placed in the center of the ring, with a compensation coil at a certain distance. When the pick up coil is properly compensated for the applied field, the integrated pick up voltage is proportional to the current in the ring. Assuming a homogeneous current distribution in the ring we can calculate the mutual inductance between the ring and the pick up coil. With this value we can determine the magnitude of the current in the ring quantitatively. The preparation of the rings and the measurement of the critical currents, using the technique described, has been used previously for the study of the influence of additives on the critical current of YBaCuO and is described elsewhere [7].

The voltage induced in the ring is proportional to the time derivative of the applied field and consequently to the frequency of the AC field (at constant amplitude). For a sinusoidal applied field the induced voltage is given by $U_{ring} = \dot{\phi}_{ring} = \dot{B}_a A_{ring} = \omega B_{ao} A_{ring}$, where A_{ring} is the effective cross section of the ring and B_{ao} is the amplitude of the applied field. By measuring the induced current in the ring as a function of the AC field frequency, the I-V characteristic of the material can be measured.

Results

A typical example of the induced current I_r in a YBaCuO ring (sample H2) as a function of the applied field B_a is shown in Fig. 4. A calculated I_r as a function of B_a is shown in Fig. 5. As we can see the shape of both curves is very similar. The main difference is that the calculated curve lies flat where the measured curve is little tilted.

The tilt has two possible causes. First it could be the result of an imperfect compensation of the signal induced by the applied field. Since the compensation is be done in situ it is not likely in this case. Secondly, because the rings are made of bulk YBaCuO they contain single crystalline grains with a higher J_c than the ring as a whole. At the position of the pick up coil the shielding currents in the grains generate a field in the same direction as the applied field. As long as the shielding currents in the grains are not saturated, i.e. as long as there is no hysterisis in the magnetization arising from the grains, the fields generated by these currents are proportional to the applied field, leading to a small tilt of the curve in Fig. 4. This effect has also been observed by Calzona et al [8].

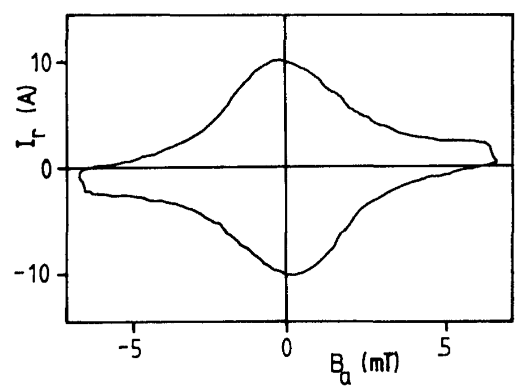

Figure 4. Current I_r as a function of applied field B_a of YBaCuO ring H2, measured at 77.3 K and a frequency of 50 Hz. The ring has an inner(outer) radius of 12.5(14.5) mm and a thickness of 2 mm.

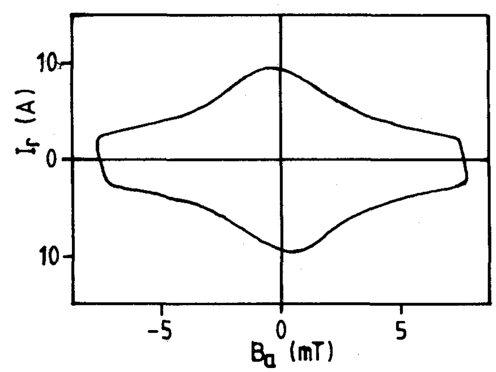

Figure 5. Calculated current I_r as a function of applied field B_a for a YBaCuO ring with inner(outer) radius of 12.5(14.5) mm and a thickness of 2 mm. The parameters used in the calculation are: $J_{co}=3\times10^7$ A/m^2, B_o = 1 mT, $\rho_n = 1\times10^{-6}$ Ωm, n = 5 and f = 1 Hz. The cross section of the ring was divided in 4×4 segments.

The frequency dependence of I_r in sample H2 has been measured between 0.1 and 50 Hz at 77.3 K. The results are shown in Fig. 6. For the field and ring used in the experiment, the induced voltage is given by $U_r \cong$ frequency × 15 μV/Hz giving an induced voltage of 300 μV at 20 Hz. The slope of the curve in Fig. 6 gives an effective n-value $n_{eff} \approx 64$.

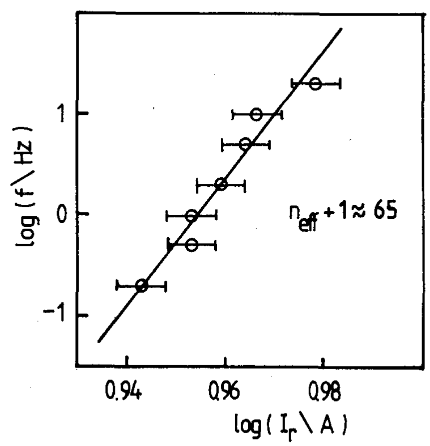

Figure 6. Experimental frequency dependence of the current I_r sample H2, measurd at 77.3 K. I_r is determined at B_a = 0 T.

Fig. 7 shows calculated frequency dependence of Ir using the parameters from Fig. 5. The induced voltage derived above compares very well with the $R_i I_i$ values obtained from the calculations. The slope of the curve in Fig. 7 gives an effective n-value $n_{eff} \approx 8$. We see that, although the magnitude of the currents and the shape of the curves in Fig. 4 and Fig. 5 are comparable, the frequency dependence of the currents is very different.

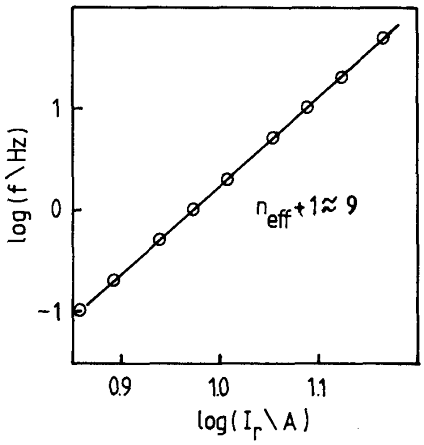

Figure 7. Calculated frequency dependence of the current I_r with the parameters in Fig. 5.

Fig. 8 shows an experimentally I-V characteristic of a YBaCuO ring, determined using a four-point method. The two curves are measured on different parts of the ring. Fig. 9 shows a logarithmic plot of curve 1 in Fig. 8. As we can see from Fig. 9 the effective n-value varies from 4 to 14 for comparable voltages as for the inductive measurments in Fig. 6. The n-values obtained from Fig. 9 are typical for the YBaCuO material.This means that the resistively and inductively determined effective n-values are not in agreement. They differ almost an order of magnitude.

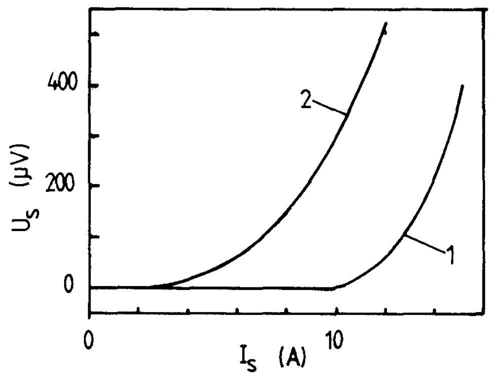

Figure 8. Experimental I-V characteristic of a YBaCuO ring, measured using a four-point technique. The two curves are measured on different parts of the sample.

From Fig. 8 we see that one sample can contain regions with different J_c. If there is a region in the ring with a lower J_c there will be a current redistribution in that region. As a result currents will only be saturated at the low J_c region but not in the rest of the ring. Furthermore, the currents will no longer be axially symmetric. The low J_c region determines the maximum current. The rest of the ring only contributes to the response of the currents to the AC field. Since the these currents are not saturated there will mainly be a redistribution of the currents. The frequency dependence will therefore be smaller than for saturated currents.

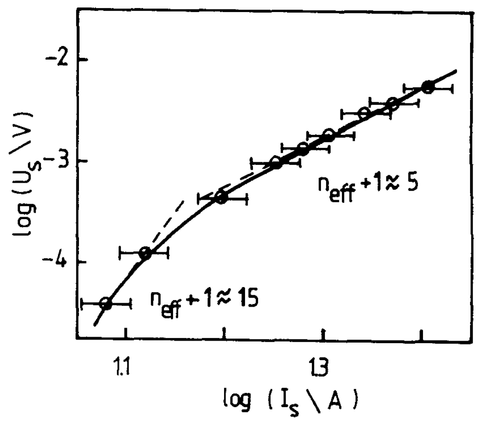

Figure 9. Logarithmic plot of I-V characteristic 1 from Fig. 8. $n_{eff} \approx 4$ at the largest currents and increases towards lower currents.

Conclusion

The shape of our AC magnetization curves is well reproduced by the model, but the frequency dependence is not. This is probably because the model cannot cope with inhomogeneities in J_c that are not in the r- or z-directions. This problem is present in all models that determine critical current densities from magnetization curves and that are based on the assumption that J_c is homogeneous. This shows that it is hazardous to infer a critical current density from the shape of AC (and DC) magnetization curves. Before determining a current density it should be checked that J_c is homogeneous.

References

1. C.P. Bean, *Rev. of Mod. Phys.*, **36**, 31, 1964.

2. M. Tinkham, *Introduction to Superconductivity*, Chap. 5.6, (Krieger, Malabar, 1980).

3. D.J. Frankel, *J. Appl Phys.*, **50**, 5402, 1979

4. M. Däumling and D.C. Larbalestier, *Phys. Rev. B*, **40**, 9350, 1989.

5. L.D. Landau and E.M. Lifshitz, *Course of theoretical Physics Volume 8, Electrodynamics of continuous media*, 2nd edition (Pergmon Press, Oxford, 1984) p. 112.

6. T.H. Fawzi and P.E. Burke, *IEEE Transactions on Power Apparatus and Systems*, vol. PAS-97, no. 2, 464, 1978.

7. A.R. Kuper, P. Hoogendam, H. Hemmes, B.H. Kolster, and L.J.M. van de Klundert, *Physica B*, **165&166**, 1365, 1990.

8. V. Calzona, M.R. Cimberle, C. Ferdeghini, F. Pupella, M. Putti, C. Rizzuto, A. Siri, and R. Vaccarone, *Cryogenics*, **30**, 569, 1990